Multi-Satellite Precipitation Products for Meteorological Drought Assessment and Forecasting in Bundelkhand region of Central India

Varsha Pandey[a], Prashant K Srivastava[a*], R K Mall[a], Francisco Munoz-Arriola[b], Dawei Han[c]

[a]*Institute of Environment and Sustainable Development and DST-Mahamana Center for Excellence in Climate Change Research, Banaras Hindu University, Varanasi, Uttar Pradesh 221005, India*

[b]*School of Natural Resources, University of Nebraska-Lincoln, USA*

[c]*Department of Civil Engineering, University of Bristol, UK*

**Corresponding author E-mail: prashant.iesd@bhu.ac.in*

Abstract

Sparse ground observation networks with minimal maintenance limit spatio-temporal coverage of precipitation data in the Bundelkhand region of Uttar Pradesh state of India, which constraint the real-time drought assessment and monitoring. In this study, comparative analysis of three satellite precipitation products including Tropical Rainfall Measuring Mission (TRMM-3B43), Precipitation Estimation from Remotely Sensed Information using Artificial Neural Networks-Climate Data Record (PERSIANN-CDR), and Climate Hazards Group InfraRed Precipitation with Station (CHIRPS version-2) with ground-measured Indian Meteorological Department (IMD) precipitation data were performed to evaluate meteorological drought in Central India. Statistical comparison was performed for nineteen years (1998-2016) at the grid level (39 grids) to assess the performance and estimate the regional differences in the spatial distribution of satellite precipitation products as compared to IMD data. The high-resolution CHIRPS showed the closest

agreement with IMD precipitation and again it well captured the drought characteristics through the Standardized Precipitation Index (SPI). There are seven major droughts events were observed in the study area between the periods of 1981 to 2016. After proper calibration and validation of the datasets, the forecasting of drought using the Auto-Regressive Integrated Moving Average (ARIMA) model in the R programming environment was also established. The best model was selected based on the ARIMA and statistical analysis such as minimum Akaike Information Criterion (AIC) and Bayesian Information Criterion (BIC). Forecasting result showed a reasonably good agreement with the observed datasets. The outcomes of this study have policy level implications for drought monitoring and prior preparedness in response to projected drought conditions using satellite data in this region.

Keywords: SPI; Meteorological drought; Precipitation; ARIMA model; Forecasting.

1. Introduction

Most of the Indian states are severely affected by recurrent and prolonged dry conditions, which significantly affect crop yield, livestock, allied sectors and thereby socioeconomic condition of the country. The prolonged dry condition leads to drought events that simply defined as the shortage in precipitation amount received over an area for an extended period of time (season or a year). It is characterized as a stochastic phenomenon with indistinct onset and ends, an undefined structure, and its slower impact that accumulated in a considerable period. Considering its complexity and nature, drought has been grouped into four types: meteorological, agricultural, hydrological, and socioeconomic (Wilhite, 2000; Wilhite and Glantz, 1985). The meteorological drought initiated due to a significant deficit of precipitation from long term climatology, which is considered as the initiator of other drought types viz., agricultural, hydrological and socioeconomic droughts (Hao and Singh, 2015; Heim Jr, 2002).

In recent years, drought events become more recurrent and severe due to global climate alteration. Numerous studies have indicated that precipitation is the precursor of onset and persistence of meteorological and other drought types. Therefore, reliable measurement of precipitation at different temporal and spatial scales is important for drought hazard assessment. Although the rain gauge observation provides accurate and long-term records, the spatial coverage is too coarse and sometimes data records are discontinued that constraint the drought assessment and monitoring accurately due to the sparse or nonhomogeneous networks with high-cost maintenance especially in developing countries. On the other hand, the satellite remote sensing-based precipitation products offer a powerful alternative data source for drought monitoring with high spatial and temporal resolutions. These satellite-based precipitation products provide global monitoring of precipitation for different hydrological and climatic applications because they fill data voids over inaccessible areas where conventional rain gauge and ground radar measurements are limited or unavailable. Based on the working principle, sensor type and their range of electromagnetic spectra used in generating the products such as microwave, Infrared and Visible data or combined, numbers of integrated observational networks, the data processing algorithms and cell size, the accuracy in different precipitation products varies greatly in one product from other. Therefore, the main attention of the scientific community is a comparative analysis of these satellite precipitation products by available ground observed data that defines the accuracy of the output where these precipitation data are being used (Alijanian et al., 2017; Moazami et al., 2013; Sharifi et al., 2016; Stisen and Sandholt, 2010; Tan et al., 2015; Yang and Luo, 2014).

The widely used indices studied for precipitation dependent drought (meteorological drought) monitoring include the Standardized Precipitation Index (SPI), which uses only precipitation data (Łabędzki, 2007; McKee et al., 1993a) and also recommended by the World Meteorological

Organization (WMO) as a compliant drought index. Moreover, SPI is also used to study various aspects of drought such as its forecasting (Mishra and Desai, 2005), intensity (Naresh Kumar et al., 2009), frequency analysis (McKee et al., 1993a), spatiotemporal analysis (SIRDAŞ and Sen, 2003; Umran Komuscu, 1999) and climate change impact studies (Dubrovsky et al., 2009). The SPI is calculated for different time scales depending on the months for which the precipitation alterations have been compared from that of the long-term average data. The 1-month (SPI1) reflects the early warning of drought conditions and is applicable in determining soil moisture and crop stress. SPI3 reflects the short to medium drought conditions and is associated with the seasonal estimation of precipitation conditions. The 6-month SPI (SPI6) indicates seasonal to medium-term drought and shows drought for different seasons provides agricultural drought estimation. Whereas, SPI12 and other higher scale SPI represent the longterm drought patterns and more applicable in determining hydrological drought (Guttman, 1998; Guttman, 1999; Livada and Assimakopoulos, 2007; Naresh Kumar et al., 2009; Svoboda et al., 2012).

The projection of drought conditions studying the past and present observations, is still a challenging task due to the stochastic nature of drought. However, such projections have high usefulness in prior preparedness via advance mitigation and management strategies, most importantly in agriculture and water resource management activities. There are several studies which relied on time series analysis method for drought projection, such as an Autoregressive Integrated Moving Average (ARIMA) models, neural network methods, exponential smoothening, etc. The ARIMA model uses a statistical approach to predict reliable drought trend by time series data with its several advantages over other techniques such as fixed structure, specificity for time series, easiness, computationally inexpensive, dependency over skill and experience of the forecaster, use of backward observations, etc.

It should be emphasized that in the current study we have used the high-resolution CHIRPS data which was not used previously in any Indian sites for drought monitoring and prediction. The specific objectives of this study are 1) to evaluate the reliability of different satellite precipitation products for meteorological drought assessment with least error in Central India, 2) to monitor meteorological drought using standardized precipitation index (SPI) in Bundelkhand-UP region for 36 years (1981-2016), and 3) to forecast future drought condition developing an ARIMA model with SPI at 3-month time scale (SPI3).

2. Site Description

The study site is the Bundelkhand region of Uttar Pradesh, India; where the socio-economic condition is primarily dependent on agriculture and allied sectors. The region comprises of seven districts and stretches between the latitude 24°18' and 26°45' N and the longitude 78°16' and 81°56' E, covering an area of around 29485.34 km^2 (**Figure** 1). The altitude in the study area ranges between 58 m to 619 m above mean sea level, with the slope from north to south. Bundelkhand region has a semi-arid climatic condition and characterized by four distinctive seasons i.e., winter, summer, monsoon, and post-monsoon. The annual average rainfall ranges from 665 mm to 1035 mm, concentrated mostly in the monsoon season (June-September: JJAS) (https://data.gov.in). Bundelkhand region lies in the dry Vindhyan plateau, plagued by underdevelopment and poverty. The region frequently experiences recurrent drought events, which aggravates the food insecurity in the region. The Bundelkhand region is a rain-fed area, where precipitation was very erratic, uncertain and have the poor supply in terms of late-onset of monsoon, early withdrawal of precipitation, etc. The water scarcity due to rainfed conditions with nutrient deficit soil and low productivity makes agriculture under-invested, risky and vulnerable. This adverse condition increased the demand for drought monitoring and effective mitigation strategies in this region.

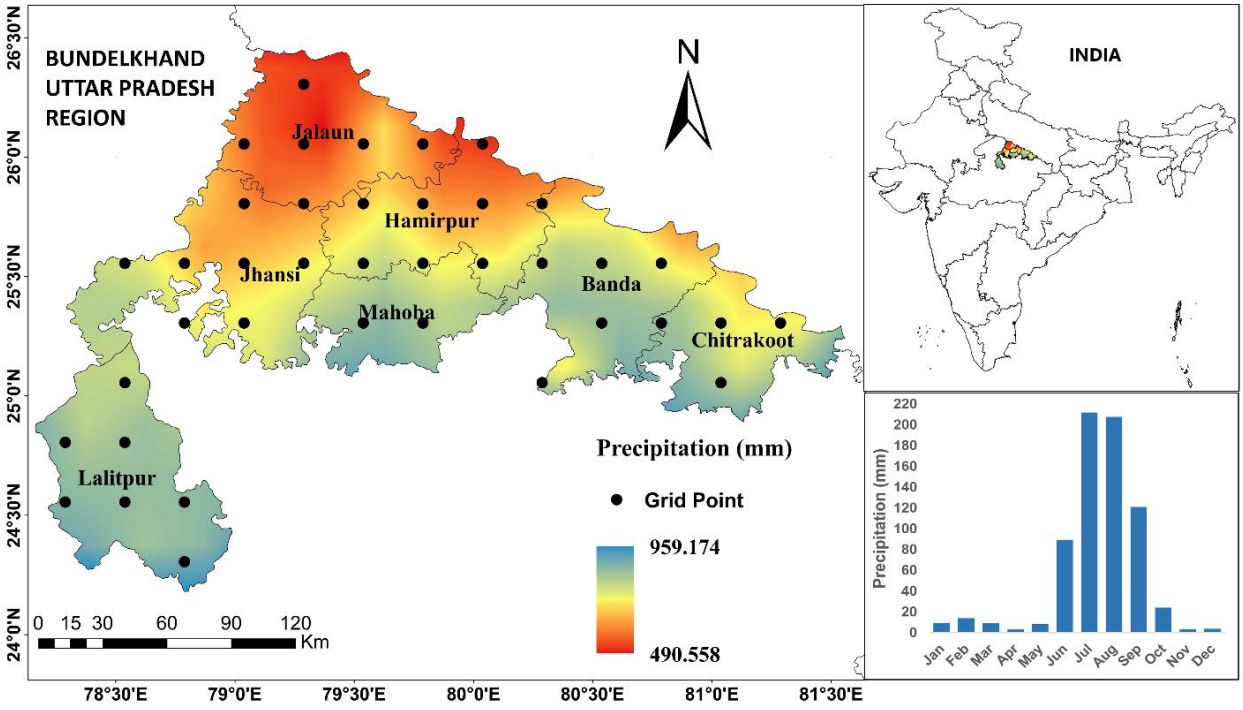

Figure 1. IMD derived study area map of mean annual precipitation between 1998 to 2016 overlaid by the IMD grid center points with monthly precipitation climatology of the Bundelkhand UP region.

3. Data and Methods

3.1. The Observed Precipitation Data

For validating satellite precipitation data products, the observed precipitation records were accessed from the archives of the National Data Center, India Meteorological Department (IMD). The daily gridded rainfall records for 116 years, from 1901 to 2016 at high spatial resolution (0.25° × 0.25°) are available for 6955 rain gauge stations over the Indian mainland. The Inverse distance weighted (IDW) interpolation technique has been employed to create continuous or precipitation gridded data (Pai et al., 2014), which has been used in the current study. Based on the available satellite precipitation data products, the IMD precipitation data during the period of 1998-2016 was used for statistical comparison with satellite precipitation data products in order to derive the

SPI for various time scale (1, 3, 6, and 12 months). The overall methodology used in this study is shown in Figure 2.

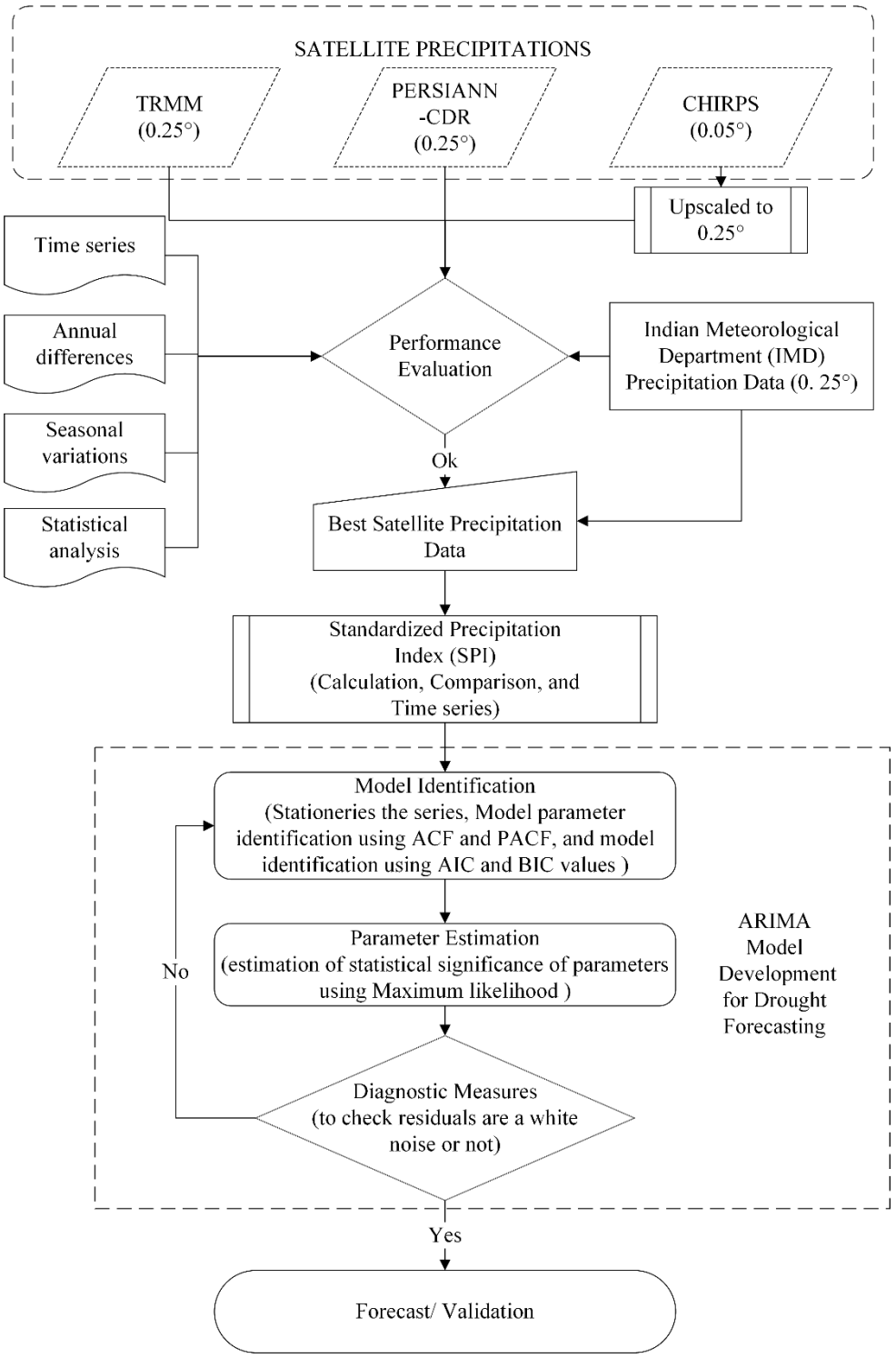

Figure 2. The workflow of the methodology

3.2. Satellite Precipitation Datasets

Three multi-satellite precipitation products namely, TRMM, CHIRPS, and PERSIANN for the period of 1998-2016, based on the availability of individual datasets, have been used in this study. The Tropical Rainfall Measuring Mission (TRMM) Multisatellite Precipitation Analysis (TMPA) 3B43 version 7 products are widely used in monitoring and studying tropical and subtropical precipitation measurements for various hydro-climatological applications such as drought assessment, flood prediction, and hydrological modeling. The widely used data product is TMPA 3-hourly 3B42 which is accumulated to daily and monthly 3B43. The TRMM products are available from 1998 to present with a high spatial resolution (0.25° × 0.25°) over near-global coverage (Huffman et al., 2007). The products were calibrated with the observed monthly precipitation rates (Liu et al., 2012). In the current study, the daily TRMM3B43 data over the study area was accessed for the analysis.

Climate Hazards Group InfraRed Precipitation with Station (CHIRPS) data is a long-term (1981-present) near-global (50°S-50°N) precipitation datasets, developed by jointly the U.S. Geological Survey (USGS) and the Climate Hazards Group (CHG) at the University of California, Santa Barbara. The thermal infrared (TIR) based high resolution (0.05°x 0.05°) CHIRPS data was developed with the main focus to support drought monitoring and forecasting and other land surface modeling activity (Funk et al., 2015). CHIRPS has relatively long precipitation records (>30 years) than other available satellite precipitation at high spatial (0.05°x 0.05°) and at daily, pentadal and monthly temporal resolution (Funk et al., 2014). It is a blended product of global precipitation climatology, geostationary TIR satellite estimates, and in-situ gauge observations ((Peterson et al., 2013). For this study, the monthly CHIRPS version 2.0 precipitation data was accessed for analysis.

156 Precipitation Estimation from Remotely Sensed Information using Artificial Neural Networks-
157 Climate Data Record (PERSIANN-CDR) is a recent multi-satellite high-resolution precipitation
158 data developed by the Center for Hydrometeorology and Remote Sensing (CHRS), University of
159 California, Irvine (UCI). The PERSIANN-CDR were generated applying artificial neural network
160 approach on GridSat-B1 infrared (IR) satellite product to provide an estimate of precipitation rate
161 at a 0.25° × 0.25° spatial resolution across the near-globe (60°N-60°S) at daily temporal resolution
162 as a high-quality Climate Data Record (CDR) of precipitation from 1983 to the near-present
163 (Ashouri et al., 2015; Miao et al., 2015). The near-global available precipitation data supports
164 many meteorological applications especially extreme events like drought and flood analysis.

165 **Table 1.** Summary of the Satellite precipitation products

Satellite Precipitation Products	Spatial Resolution	Temporal Resolution	Temporal Coverage
TRMM	0.25°	1998-Present	Daily/Monthly
PERSIANN-CDR	0.25°	1983-Present	Daily
CHIRPS	0.05°	1981-Present	Daily

166

167 **3.3. Precipitation performance evaluation**

168 The time series of monthly precipitation was prepared using spatially-aggregated data to
169 quantify the variation between the observed IMD and satellite precipitation products. The annual
170 average difference was calculated to measure the departure of monthly satellite precipitation data
171 from the observed one for each year that allowed to assess the level of underestimation and
172 overestimation of the satellite precipitation products. For accompaniment, the seasonal
173 climatological variations were also derived by temporally aggregating mean for winter (Jan-Feb;
174 JF), pre-monsoon (March-May; MAM), monsoon (June-Sept; JJAS), and post-monsoon (Oct-Dec;

175 OND) seasons during 1998 to 2016 to determine the differences in the seasonal inter-relationship
176 among satellites precipitation datasets.

177 For a comprehensive evaluation of satellite-precipitation products, a series of widely used
178 statistical metrics such as Pearson's correlation coefficient (CC), Root mean square error (RMSE),
179 Mean Absolute Error (MAE), and Relative Bias (RB) were calculated against observed gauge
180 precipitation data (**Table 2**). CC was applied to test the agreement or linear association between
181 two variables (i.e., how well satellites precipitation corresponds to the observed precipitation).
182 Whereas, the RMSE and MAE are used for measuring the average magnitude of estimated error
183 between observed and satellite precipitation with units of the variable interest. RB depicted the
184 deviation between the observed and satellite precipitation values. The overall evaluation was
185 performed by pooling all the values from the 39 point for the periods 1998-2016 and then
186 comparing with their respective grid points.

187 **Table 2.** List of statistical metrics used in the validation of satellite precipitation products
188 (CHIRPS, PERSIANN-CDR and TRMM), where "O" stands for observed precipitation, "S"
189 represents the satellite precipitation, and "n" is the sample size.

Statistical Metrics	Equation	Optimal Value	Unit
CC	$r = \frac{\sum_{i=1}^{n}(O_i - \overline{O})(S_i - \overline{S})}{\sqrt{\sum_{i=1}^{n}(O_i - \overline{O})^2}.\sqrt{\sum_{i=1}^{n}(S_i - \overline{S})^2}}$	1	-
RMSE	$RMSE = \sqrt{\frac{1}{n}\sum(S_i - O_i)^2}$	0	mm
MAE	$MAE = \frac{1}{n}\sum\lvert S_i - O_i\rvert$	0	mm

Relative Bias	$RB = \frac{\sum_{i=1}^{n}(S_i - O_i)}{\sum_{i=1}^{n}(O_i)}$	0	-

190

191 **3.4. The Standardized Precipitation Index**

192 The Standardized Precipitation Index is a climatic proxy specifically used for quantification of
193 meteorological drought (Karavitis et al., 2011). The World Meteorological Organization (WMO)
194 recommends the SPI as a versatile drought index, as it can be used for a variety of time scales and
195 conditions. Short duration SPI computation evaluates the impact of drought on agriculture, while
196 longer duration SPI is most suitable for detecting hydrological drought hazard (Vicente-Serrano et
197 al., 2014). The SPI computation required fitting a probability distribution such as the Pearson Type
198 III or Gamma probability function for homogenized long-term precipitation records to attain the
199 standard normal variable as normally it follows the nonnormal stable distribution. Then it is
200 transformed into a normal distribution with the unit standard deviation and zero mean for the
201 selected region and desire period through equiprobability transformation (Guttman, 1998).

202 In this study, we have calculated SPI on a 1-, 3-, 6-, and 12-month time scale for evaluation
203 of meteorological drought using the R platform. In agreement with previous studies, gamma
204 distribution found to be fit well to long-term precipitation records (Livada and Assimakopoulos,
205 2007; McKee et al., 1993b; Stagge et al., 2015; Thom, 1958). It is defined in terms of frequency
206 or probability density function, as follows:

207 $$g(\mathrm{x}) = \frac{1}{\beta^{\alpha}\Gamma(\alpha)} x^{\alpha-1} e^{-x/\beta} \text{ , for X>0} \quad (1)$$

where $\Gamma(\alpha)$ is the gamma function; x is the precipitation; and α and β are the shape and scale parameters respectively which estimated for each location and time scale of interest (1, 3, 6, and 12, etc.). The maximum probability for a multiyear dataset, α and β vary according to the following equation:

$$\alpha = \frac{1}{4A}\left\{1+\sqrt{1+\frac{4A}{3}}\right\}, \beta = \frac{\bar{x}}{\alpha}, \text{where} A = \ln(\bar{x}) - \frac{\sum \ln(x)}{n} \quad (2)$$

where $\bar{x}$ represents the precipitation mean and n number of observations. The cumulative probability is then computed by the obtained parameters. Since the gamma function is undefined for X=0 and a precipitation distribution may contain zeros, the cumulative probability becomes:

$$H(x) = q + (1-q)\,G(x) \quad (3)$$

The probability of no precipitation (q) is calculated by the division of m and n, as $q = m/n$. Here m is the number of the zero precipitation amount in a temporal sequence of data. The H (x) is then transformed into z score value with mean zero and unit variance, which denotes the value of the SPI. The range of SPI is varying between 2 to -2, where negative SPI value indicates drier or drought events and a positive value indicate wet events (**Table 3**).

Table 3. Drought classification based on SPI values (McKee et al., 1993a)

SPI values	Categories	Probabilities (%)
>2.0	Extremely wet	2.3
1.5 to 1.99	Very wet	4.4
1.0 to 1.49	Moderately wet	9.2
-0.99 to 0.99	Near normal	68.2
-1.0 to -1.49	Moderately dry	9.2
-1.5 to -1.99	Severe dry	4.4
<-2.0	Extremely dry	2.3

3.5. Time series model development: Autoregressive Integrated Moving Average (ARIMA)

ARIMA time series model is a structured empirical technique for forecasting and analyzing the stochastic nature of drought. When the time series data is stationary and linear, the Auto Regressive (AR) or Moving Average (MA) or mixed Auto Regressive Moving Average (ARMA) models are applied. However, when time series data is non-stationary and non-linear, the differencing is applied before the application of Auto Regressive Integrated Moving Average (ARIMA)(Contreras et al., 2003; Hamilton, 1994). The ARIMA model is mainly of two types: (a) non-seasonal linear ARIMA models that defined by parameters as ARIMA (p, d, q) and (b) multiplicative seasonal ARIMA models that is defined by adding seasonal parameters as ARIMA (p, d, q) (P, D, Q). The non-seasonal ARIMA model is mathematically expressed as (Brockwell and Davis, 2016; Wei, 2006):

$$\phi(B)\nabla^d Z_t = \theta(B)a_t \tag{4}$$

where, $\phi(B)$ and $\theta(B)$ are polynomials for p and q order, respectively and computed as:

$$\begin{aligned}\theta(B) &= 1-\theta_1 B-\ldots-\theta_q B^q \\ \phi(B) &= 1-\phi_1 B-\ldots-\phi_p B^p\end{aligned} \tag{5}$$

However, the seasonal multiplicative ARIMA model can be written as:

$$\phi_p(B)\Phi_P(B^s)\nabla^d\nabla_s^D Z_t = \theta_q(B)\Theta_Q(B^s)a_t \tag{6}$$

where, p, d, and q are the non-seasonal parameters of the model, which denotes the order of AR model, degree of differencing and the order of the MA model and P, D, Q, and *s* are the order of seasonal AR, seasonal differencing, order of seasonal MA model and the length of the season respectively. ϕ_p, Φ_P, θ_q, and Θ_Q are polynomials coefficients.

The ARIMA model development has three stages: identification, estimation, and diagnostic measures (Box et al., 2015; Chatfield, 2000; McCleary et al., 1980). In the first stage of developing the ARIMA model, exploration of time series stationarity was done. After achieving stationarity, the general form of model determined by the autocorrelation function (ACF) and partial autocorrelation functions (PACF) (http://people.duke.edu/~rnau/411home.htm). Again, the final model is selected based on penalty function statistics the Akaike information criterion (AIC) and Bayesian Information Criterion (BIC) or Schwarz-Bayesian criterion (SBC) using the following formula (Akaike, 1974; Schwarz, 1978);

$$AIC = -2\log(L) + 2k \tag{7}$$

$$BIC = -2\log(L) + k\ln(n) \tag{8}$$

where k= (p+q+P+Q) is the parameters in the model, L denotes the likelihood function of the model, and n is the number of observations.

During model parameter estimation, least-square and moment, conditional sum-of-squares or maximum likelihood functions (Wilson, 1989) were applied, where the statistical significance was qualified using various statistics like standard error, p-values, t-statistics, z-vales, etc. In the last stage of model development, the diagnosis of the ARIMA model was done to determine whether it is adequate (i.e., residuals are a white nose or not). Many diagnostic statistical test and plots of residuals are used in detection of correlation between residuals and white noise such as ACF of residuals (RACF), normal probability of residuals, Periodogram check, histograms of residuals, residuals distribution around the mean, Kolgomorov–Smirnov (K–S) tests, Ljung Box test, etc. (Box and Pierce, 1970; Li, 2003). The process is again repeated for identification if the model was not adequate and followed the above-mentioned assumptions. If all assumptions are fulfilled and diagnostic measures are satisfied, we can go for a forecast using the best fit model.

4. Results and Discussion

4.1. Precipitation Evaluation

The spatially-averaged monthly time series of observed IMD and satellite-derived precipitations are shown in **Figure 3a**. Although all the satellites follow a similar pattern, the phase shift is observed in the year 2002 between all satellite-derived precipitations and IMD data. The highest precipitation peaks are observed in TRMM and PERSIANN-CDR than CHIRPS that almost similar precipitation to the observed one with comparative lower overestimation in the rest of the years. **Figure 3b** shows the annual averaged monthly difference between the satellite precipitation products and IMD precipitation data. As similar to the previous observations, TRMM shows the highest overestimation (nearly up to 50 mm) in almost every year except 1998, 2003, 2007, 2009, and 2010; whereas, the PERSIANN-CDR shows the high difference. In comparison, CHIRPS data shows the lower difference and best fit in all the years with slight overestimation except a slight underestimation (-0.3 mm) in 2003. In addition, the significant seasonal difference of precipitation was observed during the monsoon season indicates overestimation in comparison to IMD data, which is lowest for CHIRPS followed by PERSIANN-CDR and TRMM (**Figure 3c**).

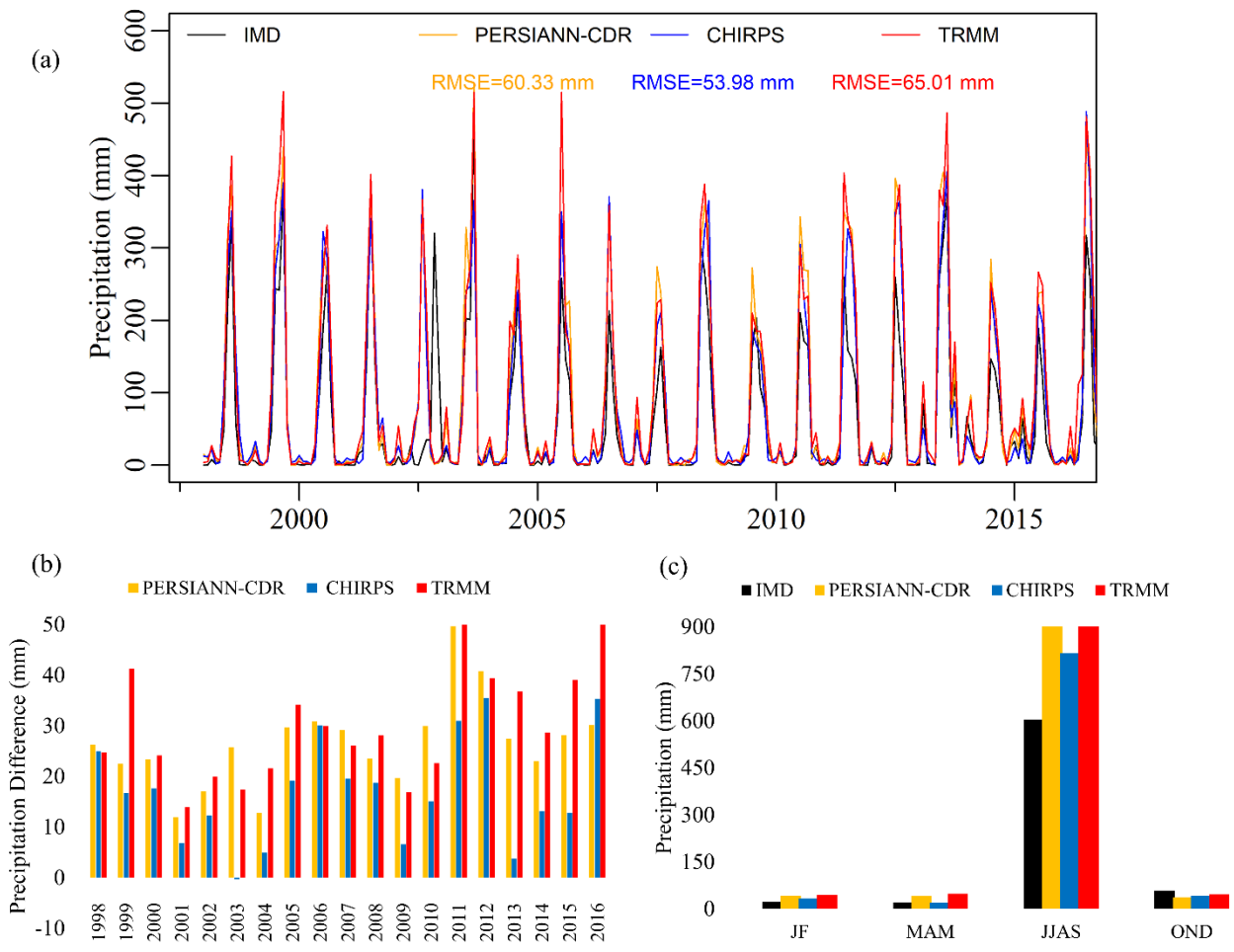

Figure 3. The monthly time series (a), Annual averaged difference (b), and Seasonal variations (c) between IMD precipitation and three satellite precipitation products

The statistical comparison between the observed IMD and satellite precipitation was carried out for individual IMD grids (39 grids) in the study area. The plots of different statistical metrics between ground observed and three different satellite precipitation estimates are shown in figure 4. All the satellite precipitation products showed good agreement with the correlation coefficient values ranging from 0.75 to 0.94. The relatively higher CC was obtained for TRMM with maximum, minimum and average values as 0.94, 0.79 and 0.88, respectively, followed by PERSIANN-CDR (0.93, 0.76 and 0.88) and CHIRPS (0.92, 0.75 and 0.87) (**Figure 4a**). However, all satellite precipitation seems to overestimate the monthly ground observed precipitation for all

the points except 13 where PERSIANN-CDR underestimated the precipitation. CHIRPS showed a minimum relative bias score of 0.58 that was closest to the perfect score of zero in comparison to TRMM (0.81) and PERSIANN-CDR (0.99) (**Figure 4b**). In addition, CHIRPS performed well in terms of MAE and RMSE with an average score of 31.99 mm month^{-1} and 60.68 mm month^{-1}, respectively for all the validation points. Whereas, the MAE for PERSIANN-CDR and TRMM were estimated as 35.90 mm month^{-1} and 37.60 mm month^{-1} with the RMSE values of 67. 35 mm month^{-1} and 71.57 mm month^{-1}, respectively (**Figure 4c, d**).

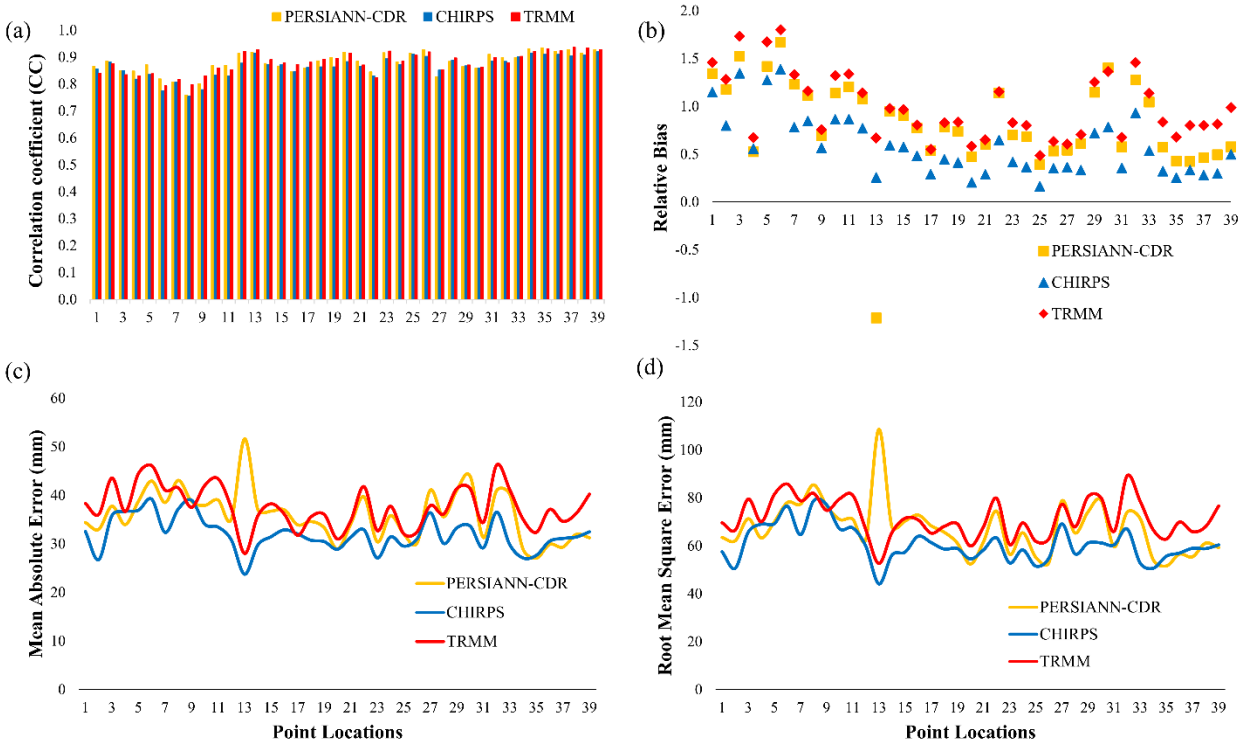

Figure 4. The statistical metrics- correlation coefficient (a), Relative bias (b), Mean absolute error (c), and Root mean square error (d)- for the selected 39 points in the study area.

The scatter plot between observed IMD precipitation and the three satellite products (TRMM, CHIRPS, and PERSIANN-CDR) for the nineteen-year monthly precipitation for 39 points over the Bundelkhand region is shown in **Figure 5**. All satellite products showed a

significant ($p < 0.0001$) coefficient of determinants (R^2), which was comparatively higher for TRMM (0.78) followed by PERSIANN-CDR (0.77) than CHIRPS (0.75) at 95 % confidence level. However, the regression line exhibited the closest agreement with 1:1 line for CHIRPS followed by PERSIANN-CDR and TRMM, which also indicates their relative bias errors. **Table 4** summerise all the statistics used in the evaluation of satellite products. The overall performance of all three satellite products is promising for identifying precise satellite precipitation products that could potentially be utilized in meteorological drought monitoring. However, the statistical comparison shows a comparatively better correlation coefficient for TRMM and PERSIANN-CDR in almost all the points, the CHIRPS exhibits the lowest error in terms of MAE, RMSE, and bias that indicates better performance of CHIRPS in comparison to TRMM and PERSIANN-CRD. Thus, we have selected high-resolution CHIRPS data in this study for meteorological drought assessment and forecasting in the Bundelkhand region.

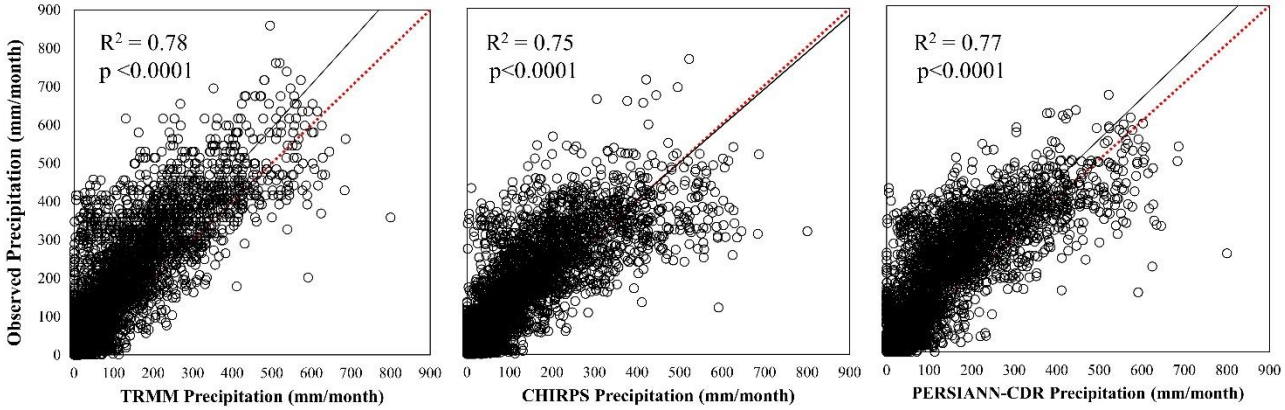

Figure 5. Scatter plots between the observed IMD precipitation and the three satellite-based precipitation at a monthly time scale. Linear regression is fitted with sample size (n) 8892. The dashed red line indicates 1:1 and the black line indicates the best fit linear regression line.

Table 4. Summary of statistical metrics

Data sets	PERSIANN-CDR	CHIRPS	TRMM
R^2	0.77	0.75	0.78
CC	0.88	0.87	0.88
RB	0.81	0.58	0.99
MAE	35.90	32.00	37.60
RMSE	67.35	60.68	71.57

4.2. SPI Comparison

Additionally, we further corroborated the suitability of CHIRPS in drought monitoring applications. The spatially averaged SPI has been calculated at different timescales as SPI1, SPI3, SPI6, and SPI12 to compare with IMD derived SPI from 1998 to 2016 (**Figure 6**). The SPI is computed by the domain-averaging process, for the purpose of the SPI comparison to assess the accuracy of CHIRPS product as a proxy for drought monitoring rather than reflecting drought conditions over the study area. We observed close agreements and consistency between CHIRPS and IMD data derived SPI values in terms of both frequency and intensity. CHIRPS performs well in capturing drought for all the time scales. It also identifies historic drought occurs in most of the Indian regions in the years 2002, 2009, 2014 and 2015 (www.iwmi.cgiar.org/; www.im4change.org/), (Gupta and Head; Samra, 2004). The correlation coefficient (r) between IMD and CHIRPS derived SPIs were estimated > 0.75 and RMSEs < 0.70 for all time scales. A comparative study among all the time scale exhibits better agreements for SPI3 and SPI6 (CC: 0.84 and 0.83 respectively; and RMSE: 0.57 and 0.59, respectively). On the contrary, SPI1 and SPI12 showed comparatively moderate and lower agreement (CC: 0.8 and 0.77, respectively and RMSE: 0.64 and 0.68, respectively). The scatter plot between observed IMD precipitation and the CHIRPS derived SPI at different time scales shown in **Figure 7.** All SPI timescale showed significant ($p<0.0001$) R^2, which was comparatively higher for SPI3 (0.71) with the comparatively

closest agreement between 1:1 and the regression line. Overall, it can infer that CHIRPS performs well in monitoring the meteorological drought in the region.

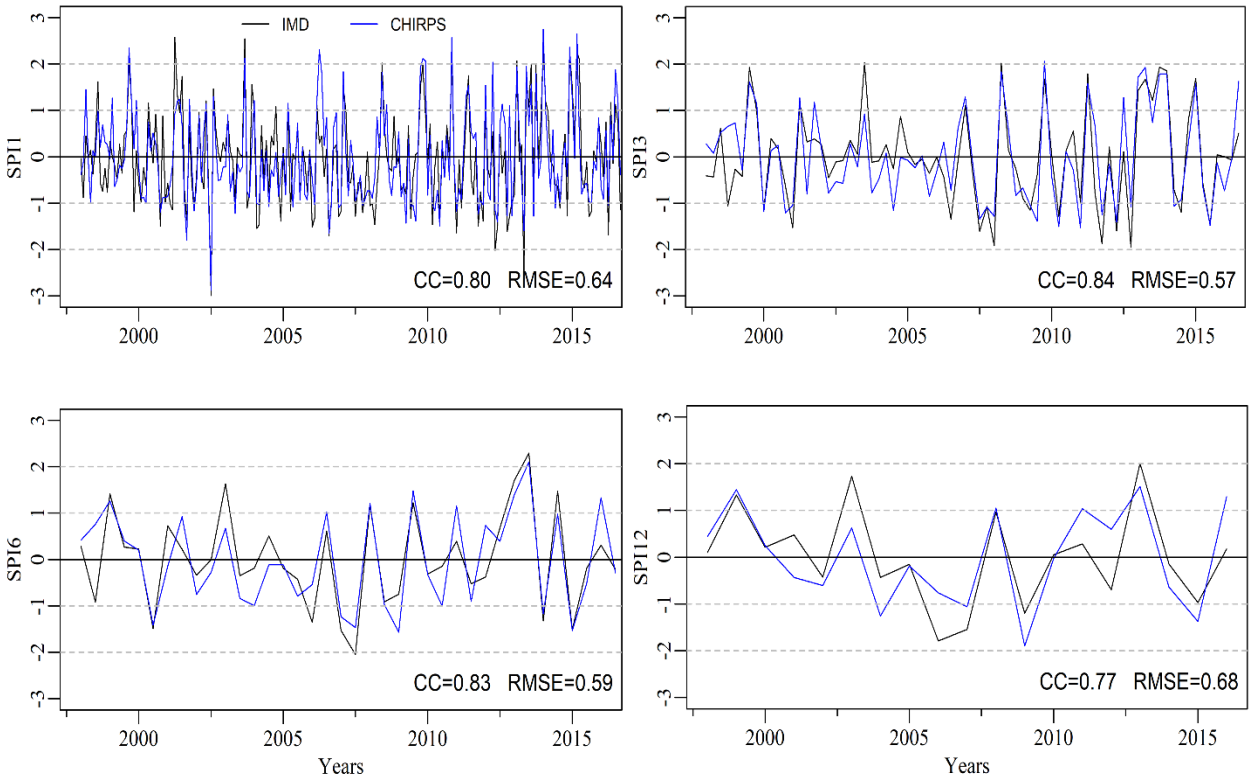

Figure 6. The SPI time series for comparison between CHIRPS and observed IMD precipitation from 1998 to 2016 at different time scales: (a) 1-month; (b) 3-month; (c) 6-month; and (d) 12-month.

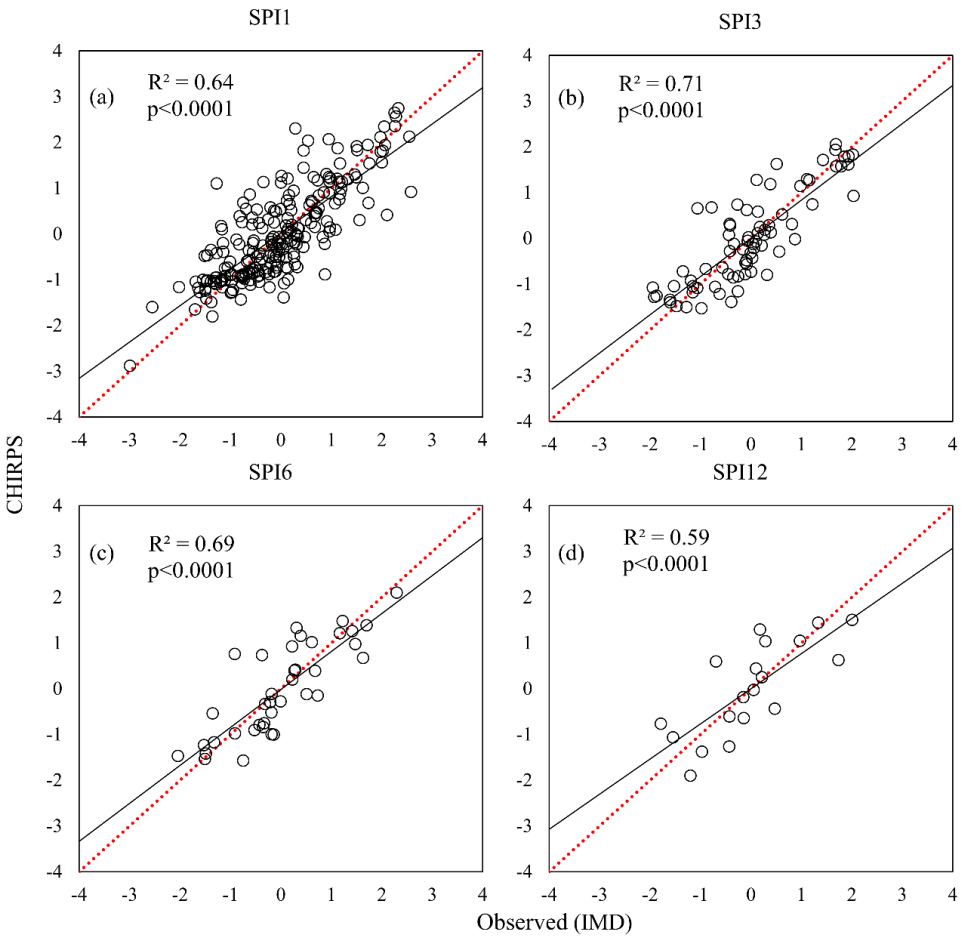

Figure 7. Scatter plots between CHIRPS and observed IMD derived SPI from 1998 to 2016 at different time scales: (a) 1-month; (b) 3-month; (c) 6-month; and (d) 12-month.

4.3. Meteorological drought assessment based on CHIRPS during Monsoon Season

The majority of the precipitation in this region is dominated in the monsoon season (June-September, JJAS). Thus, in this section, historical time-series of geographically aggregated SPI derived from the CHIRPS 2.0 precipitation data is evaluated for monsoon season during the period of 1981 to 2016 (36 years) at 3-month time scale (SPI3). In this study, SPI3 is used for defining drought patterns during the study period., indicates the drought severity was significant in several years. The obtained results suggested the occurrences of seven severe to extreme drought events in the study region between the period of 1981 to 2016 (**Figure 8**). With reference to past studies,

the years 1982, 1984, 1987 and 2014-2015 faces severe and years 1992, 2002 and 2009 faces extreme drought conditions with an intensity ranging from -1.75 to -1.87 and -2.21 to -2.30, respectively (Pandey and Srivastava, 2018; Pandey and Srivastava, 2019; Thomas et al., 2016; Thomas et al., 2015).

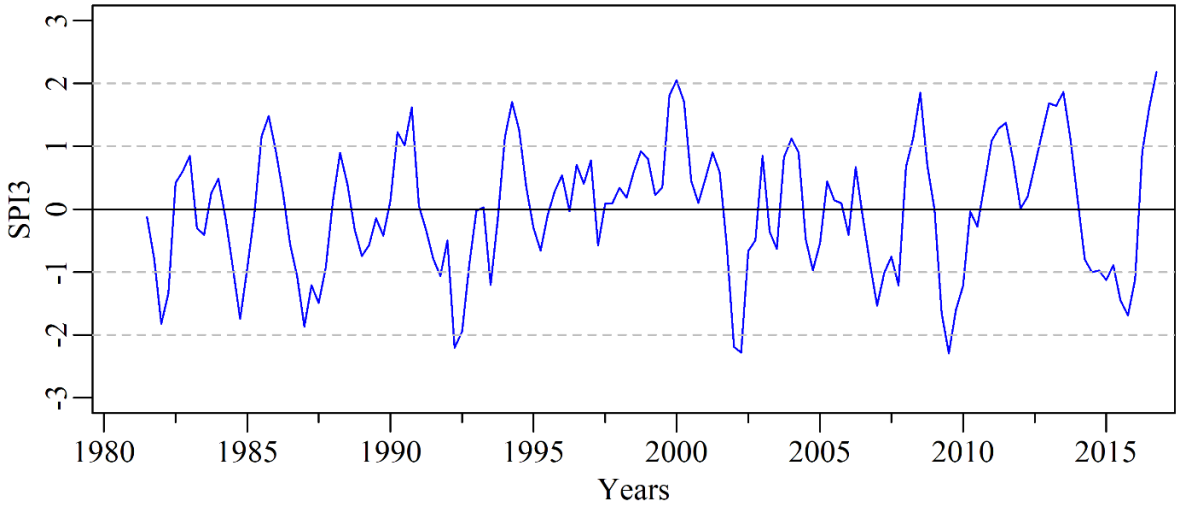

Figure 8. SPI3 time series based on all grids average over the Bundelkhand region.

4.4. SPI Time Series Modelling

4.4.1. Model Development

As drought events are stochastic in nature, it is difficult to forecast. However, the reliable forecasting of drought facilitates significant advantages for water, agriculture and disaster managers in prior mitigation strategies. The ARIMA model was used to study and forecast SPI employing the high-resolution CHIRPS data at a 3-month time scale (SPI3). The seasonal datasets (June-September: JJAS) from 1981 to 2011 were used for model development and from 2012 to 2016 were used in model validation.

4.4.1.1. Model Identification

The ACF and PACF plots generated using the SPI3 time series data are shown in **Figure 9**, suggest the input data series to be stationary. Again, the stationarity of the data series was also confirmed by applying the Dickey-Fuller Test (p = 0.01). The ACF shows a sine-wave shape with the first three significant lags and PACF with the first two significant lags, which indicates the applicability of both AR and MA components. Considering this, ARIMA (p, 0, q) model were identified with possible p = 1 to 2 and q =1 to 3. All the possible combinations were tested and compared to identify the best fit model based on minimum AIC and SBC/BIC values, which indicates white noise residuals. **Table 5** shows the different combinations of the model with estimated AIC and BIC values.

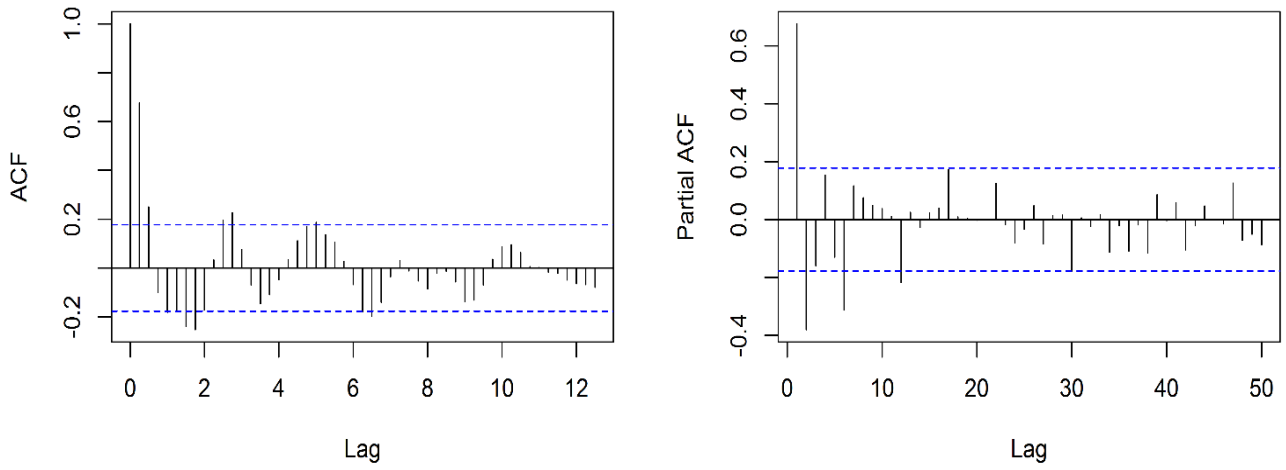

Figure 9. ACF and PACF plots used for model selection for the SPI3 series.

4.4.1.2. Parameter estimation

The second stage of model development is the estimation of parameters using the maximum likelihood method in this study. The z-values, p-values, and standard error corresponds to each parameter were evaluated to test the statistical significance of the parameters. Usually, p-

values are informative by itself and state parameters are significant if its value is less than 0.05 at a 95% confidence interval. The summary of the statistical parameters of the best fit model has been given in **Table 6**.

Table 5. Comparison of AIC and BIC for the selection of a best-fit model for SPI3.

ARIMA Models	AIC	BIC/SBC
ARIMA (2,0,0)	254.87	266.08
ARIMA (2,0,1)	254.62	268.63
ARIMA (2,0,2)	241.90	258.71
ARIMA (2,0,3)	242.78	262.41
ARIMA (1,0,3)	238.14	252.95
ARIMA (1,0,2)	243.12	257.13
ARIMA (1,0,1)	262.89	274.10
ARIMA (0,0,3)	241.60	255.62
ARIMA (0,0,2)	243.27	254.48
ARIMA (0,0,2) (0,0,1)	238.84	252.86

Table 6. Summary of the statistical parameters of ARIMA (1,0,3).

Model Parameters	Variables in the model			
	Estimate value	Standard error	Z-value	P <0.05
AR1	-0.7483	0.1221	-6.1327	0.00
MA1	1.7199	0.1052	16.3337	0.00
MA2	1.5066	0.1294	11.6376	0.00
MA3	0.7307	0.0808	9.0351	0.00
Intercept	-0.0383	0.1541	-0.2487	

4.4.1.3. Diagnostic measures

Diagnostic checking is the final and crucial step of model development that involves verification of the adequacy of the selected model using diagnostic statistics and plots of residuals. In the present study, the residual ACF function (RACF), histogram of residuals, Ljung Box test, and normal probability of residuals test were tested for residual checking. In RACF plot, the

correlogram was drawn by plotting residual ACF (r_k) against lag k. The ACF of residuals for the ARIMA (1,0,3) model is shown in **Figure 10a**. The figure indicates that all values were within the significant bounds and shown no significant correlation between residuals except the first lag. Histograms of residuals for the same model are shown in **Figure 10b**. Histograms show the normal distribution of residuals that signifies the residuals were white noise. The p-values obtained from the Ljung Box test are shown in **Figure 10c**, represents all values that were well above 0.05, indicating white noise residuals and model adequacy. The normal probability of residuals plot (**Figure 10d**) shows the white noise residuals as it appears fairly linear that holds normality assumptions of the residuals (Box and Pierce, 1970; Chow et al., 1988; Durbin, 1960; McLeod and Li, 1983).

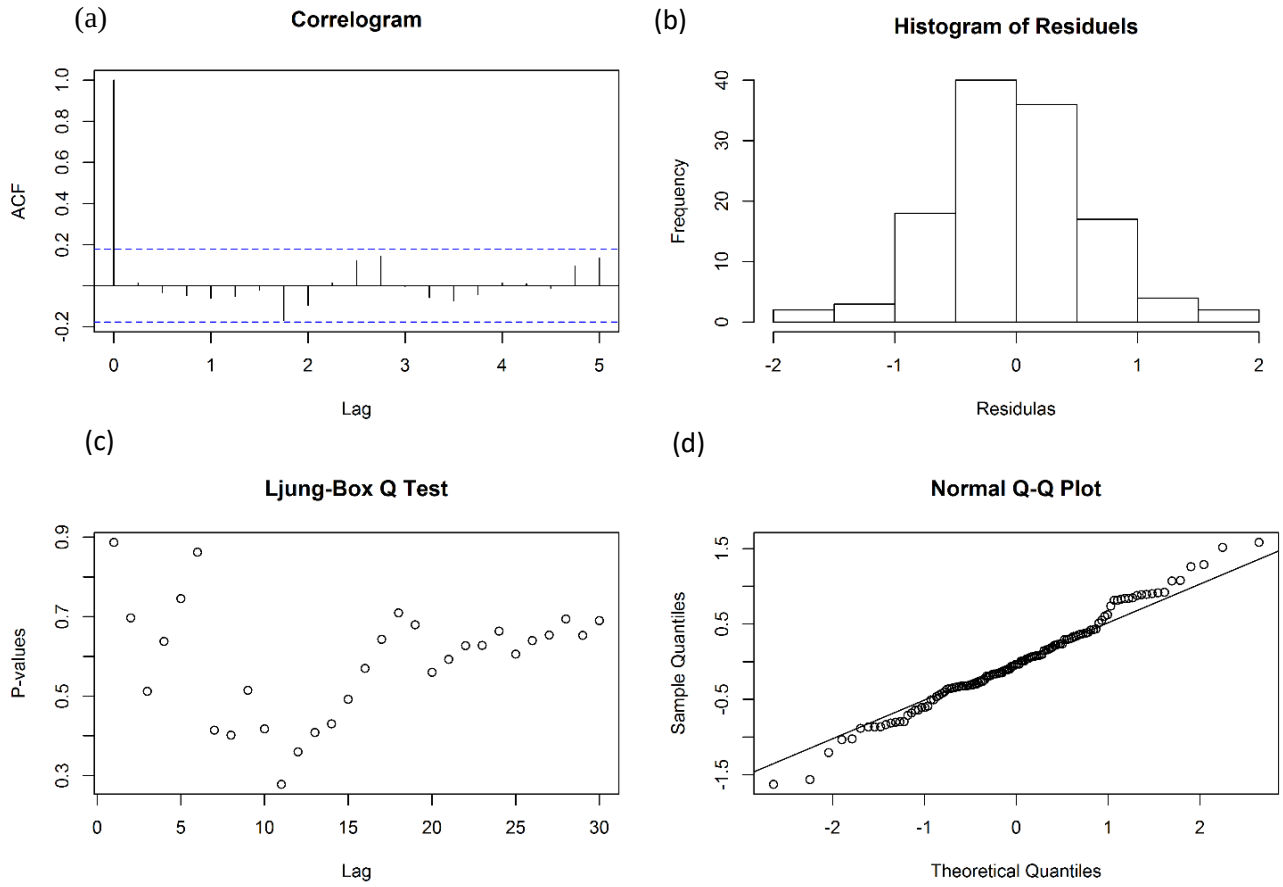

Figure 10. Diagnostic check for best-fitted model ARIMA (1,0,3)

4.4.2. Forecasting

The best fit ARIMA model (1,0,3) was validated with the observed data for the monsoon season (JJAS) from 2012 to 2016. The forecasting was done for one-month lead-time (because it decreases with increasing lead time) for better accuracy as already established by the results of Mishra and Desai (2005), Fathabadi et al. (2009), Bazrafshan et al. (2015) and Han *et al.* (2012). 1-month lead-time forecasting indicates projection for the next 1 period or time-step. **Figure 11** represents the close agreement of predicted data with both monitored (CHIRPS) and observed (IMD) data using the best fit ARIMA model for SPI3. The obtained result shows that forecasted data follows the same pattern and satisfied the basic statistics compared to the monitored and observed data. The high correlations and low RMSE are obtained for both CHIRPS and IMD (CC: 0.92 and 0.91, respectively and RMSE: 0.41 and 0.56, respectively) data.

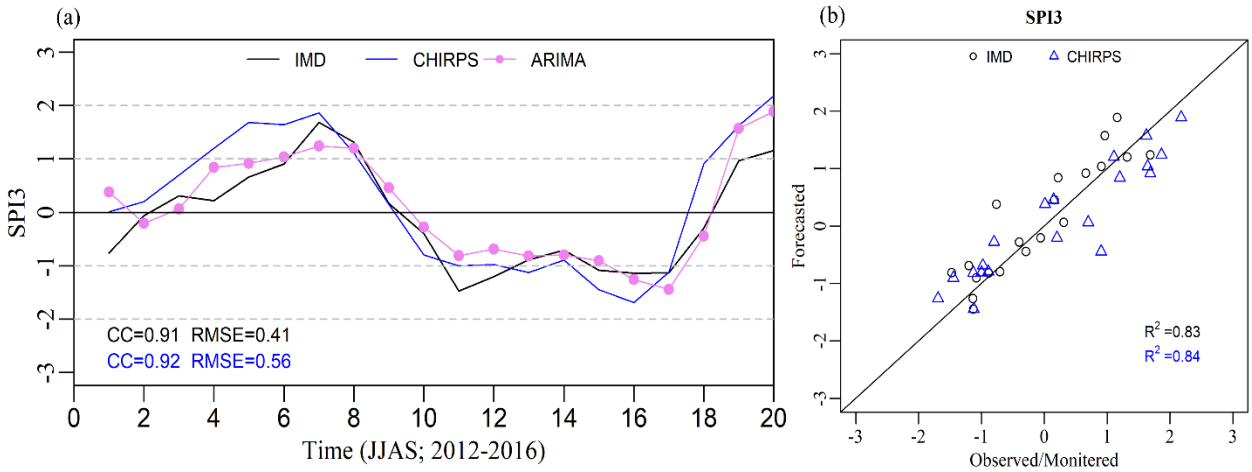

Figure 11. SPI time series (a), and scatter plot (b) for the comparison of observed (IMD and monitored by CHIRPS) with the forecasted data using the ARIMA (1,0,3) model.

5. Discussion

Evaluation of multi-satellite precipitation data has been carried out in many studies mostly at global (Beck et al., 2017; Zhao and Ma, 2019); continental (Awange et al., 2016; Kimani et al., 2017; Peña-Arancibia et al., 2013; Xie et al., 2007); country (Alijanian et al., 2017; Miao et al., 2015; Prakash, 2019; Shen et al., 2010); and regional scale (Gao and Liu, 2012; Hirpa et al., 2010; Jiang et al., 2012). However, the accuracy of such data at the local scale is less examined. In India, this is the first study which evaluates precipitation products to monitor and forecast drought hazard in relatively small Bundelkhand region that is affected by recurrent and severe drought events. This study assessed the performance of three widely used satellite-derived precipitation products having long-term records as TRMM, PERSIANN-CDR, and CHIRPS. The ground observed data recorded by IMD over this region was taken as the reference or baseline data for comparison. These evaluations are done for promoting the use of satellite precipitation products for hydro-meteorological, agriculture, natural hazards, and other related studies and planning. The evaluation was done on a monthly scale with the common grid size among the data (0.25º). Additionally, the drought evaluation was also carried out using the standardized precipitation index (SPI) a World Meteorological Organization (WMO) recommended drought index (Hayes et al., 2011). The SPI time series analysis was performed using the ARIMA model to project the SPI for drought hazard preparedness in the study region. Although the precipitation event is dependent on many dynamic and coupled processes, the SPI time series analysis was performed using the ARIMA model to project the SPI for drought hazard preparedness in the study region.

The comparison of the three multi-satellite precipitation products shows that all the three precipitation products had almost similar correlations (ranges from 0.75 to 0.94) but notable low relative bias and RMSE values (0.58 and 60.6 mm month^{-1}) are observed for CHIRPS data.

Therefore, we concluded that the satellite precipitation record is well captured by the CHIRPS data in comparison to the other two satellite precipitations data in the study region. Recent studies at India level by Prakash (2019) indicates a higher error (high bias and RMSE, and lower correlation) in satellite precipitation data (including CHRIPS) over a tropical and mountainous region in comparison to sub-tropical to the arid region including the current study area as Bundelkhand region. Over the central India region, Prakash (2019) estimated the CC as 0.99 with 0.84 (mm day^{-1}) RMSE and 1.11 bias ratio. Moreover, many studies have been also indicated CHIRPS as the best data for drought monitoring with relatively lower error and high correlation after comparing it with gauge precipitation data (Bayissa et al., 2017).

The reasonably good results of CHIRPS are probably due to its higher spatial resolutions (in account to other data having a spatial resolution of 0.25°) and integrates more in-situ data with high-resolution climatology and multi-satellite products. It was observed higher resolution is generally directly proportional to accuracy but also relied on the method employed for the generation of products (Dandridge et al., 2019). Thus, this study confirms that CHIRPS products can be used for long-term drought events variability assessment with higher confidence.

6. Conclusions

Bundelkhand region of Central India is affected by recurrent and severe meteorological drought events, which becomes worse due to poor management strategies in this underdeveloped, disregarded and economically backward region. The lack of rain gauge stations and their maintenance limits the study of meteorological drought characteristics in this region. The current study investigated the effectiveness of the three remote sensing data to monitor and forecast drought events. Results showed that the latest high resolution (0.05°) CHIRPS satellite data is the most suitable for drought characterization according to statistical performance measure tested with

480 39 grid points for the periods of 1998-2016. The monthly CHIRPS data was used to evaluate the
481 drought condition for 38 years (1981-2016) at 3- month time scale (SPI3). This research also
482 examined the feasibility of applying the ARIMA time series model using SPI3 for drought
483 forecasting in this region. The main findings of this research are as follows:

484 1) Among the three-satellite data (PERSIANN-CDR, CHIRPS, and TRMM), CHIRPS show
485 comparatively better performance in comparison to IMD observed precipitation data.
486 CHIRPS shows the closest agreement with observed data with average CC values (0.87)
487 and relatively low RB, MAE, and RMSE (0.58, 32.00 mm month^{-1}, and 60.68 mm month^{-}
488 ^{1}).

489 2) CHIRPS performs well in estimating drought condition at different SPI timescale
490 comparing with IMD observed SPI series. The three-month SPI (SPI3) has the best
491 performance with high R^2 (0.84) and low RMSE (0.57) while SPI12 shows relatively poor
492 performance.

493 3) SPI3 time series data indicates seven distinct drought events in the Bundelkhand UP region
494 at the monsoon season during 1981-2016. The four severe (in the year 1982, 1984, 1987
495 and 2015) and three extremes (in the year 1992, 2002 and 2009) drought event was
496 observed with an intensity ranging from -1.75 to -1.87 and -2.21 to -2.30, respectively.

497 4) The time series ARIMA model developed for SPI3 series based on the correlation methods
498 of Box and Jenkins and lower AIC and BIC selection criteria. ARIMA (1,0,3) was found
499 as the best fit model and detected well accurately as compared with observed data during
500 validation. The forecasting was done for a one-month lead-time indicates good accuracy.

501 This study demonstrated the usefulness of the latest CHIRPS satellite data in less or no rain
502 gauges area in the monitoring and forecasting of drought characteristics and lay the foundation for

the management of sustainable water resources, irrigation pattern, and other watershed management activities with the alike hydro-climatic conditions.

Acknowledgments

We are thankful to anonymous reviewers for their time and feedback on the manuscript. The authors are thankful to the SERB-DST and Banaras Hindu University for providing the seed grant for this research. The authors thank the India Meteorological Department (IMD), Pune, India for providing the hydrometeorological data used for validation in this study.

References

Akaike, H., 1974. A new look at the statistical model identification, Selected Papers of Hirotugu Akaike. Springer, pp. 215-222.

Alijanian, M., Rakhshandehroo, G.R., Mishra, A.K., Dehghani, M., 2017. Evaluation of satellite rainfall climatology using CMORPH, PERSIANN-CDR, PERSIANN, TRMM, MSWEP over Iran. International Journal of Climatology, 37(14): 4896-4914.

Ashouri, H. et al., 2015. PERSIANN-CDR: Daily precipitation climate data record from multisatellite observations for hydrological and climate studies. Bulletin of the American Meteorological Society, 96(1): 69-83.

Awange, J. et al., 2016. Uncertainties in remotely sensed precipitation data over Africa. International Journal of Climatology, 36(1): 303-323.

Bayissa, Y., Tadesse, T., Demisse, G., Shiferaw, A., 2017. Evaluation of satellite-based rainfall estimates and application to monitor meteorological drought for the Upper Blue Nile Basin, Ethiopia. Remote Sensing, 9(7): 669.

Bazrafshan, O., Salajegheh, A., Bazrafshan, J., Mahdavi, M., Fatehi Maraj, A., 2015. Hydrological drought forecasting using ARIMA models (case study: Karkheh Basin). Ecopersia, 3(3): 1099-1117.

Beck, H.E. et al., 2017. Global-scale evaluation of 22 precipitation datasets using gauge observations and hydrological modeling. Hydrology and Earth System Sciences, 21(12): 6201-6217.

Box, G.E., Jenkins, G.M., Reinsel, G.C., Ljung, G.M., 2015. Time series analysis: forecasting and control. John Wiley & Sons.

Box, G.E., Pierce, D.A., 1970. Distribution of residual autocorrelations in autoregressive-integrated moving average time series models. Journal of the American statistical Association, 65(332): 1509-1526.

Brockwell, P.J., Davis, R.A., 2016. Introduction to time series and forecasting. springer.

Chatfield, C., 2000. Time-series forecasting. Chapman and Hall/CRC.

Chow, V.T., Maidment, D.R., Mays, L.W., 1988. Applied hydrology.
Contreras, J., Espinola, R., Nogales, F.J., Conejo, A.J., 2003. ARIMA models to predict next-day electricity prices. IEEE transactions on power systems, 18(3): 1014-1020.
Dandridge, C., Lakshmi, V., Bolten, J., Srinivasan, R., 2019. Evaluation of Satellite-Based Rainfall Estimates in the Lower Mekong River Basin (Southeast Asia). Remote Sensing, 11(22): 2709.
Dubrovsky, M. et al., 2009. Application of relative drought indices in assessing climate-change impacts on drought conditions in Czechia. Theoretical and Applied Climatology, 96(1-2): 155-171.
Durbin, J., 1960. The fitting of time-series models. Revue de l'Institut International de Statistique: 233-244.
Fathabadi, A., Gholami, H., Salajeghe, A., Azanivand, H., Khosravi, H., 2009. Drought forecasting using neural network and stochastic models. Advances in Natural and Applied Sciences, 3(2): 137-146.
Funk, C. et al., 2015. The climate hazards infrared precipitation with stations—a new environmental record for monitoring extremes. Scientific data, 2: 150066.
Funk, C.C. et al., 2014. A quasi-global precipitation time series for drought monitoring. US Geological Survey Data Series, 832(4): 1-12.
Gao, Y., Liu, M., 2012. Evaluation of high-resolution satellite precipitation products using rain gauge observations over the Tibetan Plateau. Hydrology & Earth System Sciences Discussions, 9(8).
Gupta, A.K., Head, N., Vulnerability Assessment and Mitigation Analysis for Drought in Bundelkhand Region.
Guttman, N.B., 1998. Comparing the Palmer drought index and the standardized precipitation index. JAWRA Journal of the American Water Resources Association, 34(1): 113-121.
Guttman, N.B., 1999. Accepting the standardized precipitation index: a calculation algorithm. JAWRA Journal of the American Water Resources Association, 35(2): 311-322.
Hamilton, J.D., 1994. Time series analysis, 2. Princeton university press Princeton, NJ.
Han, P. et al., 2012. Application of the ARIMA models in drought forecasting using the standardized precipitation index, International Conference on Computer and Computing Technologies in Agriculture. Springer, pp. 352-358.
Hao, Z., Singh, V.P., 2015. Drought characterization from a multivariate perspective: A review. Journal of Hydrology, 527: 668-678.
Hayes, M., Svoboda, M., Wall, N., Widhalm, M., 2011. The Lincoln declaration on drought indices: universal meteorological drought index recommended. Bulletin of the American Meteorological Society, 92(4): 485-488.
Heim Jr, R.R., 2002. A review of twentieth-century drought indices used in the United States. Bulletin of the American Meteorological Society, 83(8): 1149-1165.
Hirpa, F.A., Gebremichael, M., Hopson, T., 2010. Evaluation of high-resolution satellite precipitation products over very complex terrain in Ethiopia. Journal of Applied Meteorology and Climatology, 49(5): 1044-1051.
Huffman, G.J. et al., 2007. The TRMM multisatellite precipitation analysis (TMPA): Quasi-global, multiyear, combined-sensor precipitation estimates at fine scales. Journal of hydrometeorology, 8(1): 38-55.

Jiang, S. et al., 2012. Comprehensive evaluation of multi-satellite precipitation products with a dense rain gauge network and optimally merging their simulated hydrological flows using the Bayesian model averaging method. Journal of Hydrology, 452: 213-225.
Karavitis, C.A., Alexandris, S., Tsesmelis, D.E., Athanasopoulos, G., 2011. Application of the standardized precipitation index (SPI) in Greece. Water, 3(3): 787-805.
Kimani, M., Hoedjes, J., Su, Z., 2017. An assessment of satellite-derived rainfall products relative to ground observations over East Africa. Remote sensing, 9(5): 430.
Łabędzki, L., 2007. Estimation of local drought frequency in central Poland using the standardized precipitation index SPI. Irrigation and Drainage, 56(1): 67-77.
Li, W.K., 2003. Diagnostic checks in time series. Chapman and Hall/CRC.
Liu, Z., Ostrenga, D., Teng, W., Kempler, S., 2012. Tropical Rainfall Measuring Mission (TRMM) precipitation data and services for research and applications. Bulletin of the American Meteorological Society, 93(9): 1317-1325.
Livada, I., Assimakopoulos, V., 2007. Spatial and temporal analysis of drought in Greece using the Standardized Precipitation Index (SPI). Theoretical and applied climatology, 89(3-4): 143-153.
McCleary, R., Hay, R.A., Meidinger, E.E., McDowall, D., 1980. Applied time series analysis for the social sciences. Sage Publications Beverly Hills, CA.
McKee, T.B., Doesken, N.J., Kleist, J., 1993a. The relationship of drought frequency and duration to time scales, Proceedings of the 8th Conference on Applied Climatology. American Meteorological Society Boston, MA, pp. 179-183.
McKee, T.B., Doesken, N.J., Kleist, J., 1993b. The relationship of drought frequency and duration to time scales, Proceedings of the 8th Conference on Applied Climatology. American Meteorological Society Boston, MA, pp. 179-183.
McLeod, A.I., Li, W.K., 1983. Diagnostic checking ARMA time series models using squared-residual autocorrelations. Journal of time series analysis, 4(4): 269-273.
Miao, C., Ashouri, H., Hsu, K.-L., Sorooshian, S., Duan, Q., 2015. Evaluation of the PERSIANN-CDR daily rainfall estimates in capturing the behavior of extreme precipitation events over China. Journal of Hydrometeorology, 16(3): 1387-1396.
Mishra, A., Desai, V., 2005. Drought forecasting using stochastic models. Stochastic Environmental Research and Risk Assessment, 19(5): 326-339.
Moazami, S., Golian, S., Kavianpour, M.R., Hong, Y., 2013. Comparison of PERSIANN and V7 TRMM Multi-satellite Precipitation Analysis (TMPA) products with rain gauge data over Iran. International journal of remote sensing, 34(22): 8156-8171.
Naresh Kumar, M., Murthy, C., Sesha Sai, M., Roy, P., 2009. On the use of Standardized Precipitation Index (SPI) for drought intensity assessment. Meteorological applications, 16(3): 381-389.
Pai, D. et al., 2014. Development of a new high spatial resolution (0.25× 0.25) long period (1901–2010) daily gridded rainfall data set over India and its comparison with existing data sets over the region. Mausam, 65(1): 1-18.
Pandey, V., Srivastava, P., 2018. Integration of satellite, global reanalysis data and macroscale hydrological model for drought assessment in sub-tropical region of india. Int. Arch. Photogramm. Remote Sens. Spat. Inf. Sci, 42.
Pandey, V., Srivastava, P.K., 2019. Integration of Microwave and Optical/Infrared Derived Datasets for a Drought Hazard Inventory in a Sub-Tropical Region of India. Remote Sensing, 11(4): 439.

Peña-Arancibia, J.L., van Dijk, A.I., Renzullo, L.J., Mulligan, M., 2013. Evaluation of precipitation estimation accuracy in reanalyses, satellite products, and an ensemble method for regions in Australia and South and East Asia. Journal of Hydrometeorology, 14(4): 1323-1333.

Peterson, P. et al., 2013. The Climate Hazards group InfraRed Precipitation (CHIRP) with Stations (CHIRPS): Development and Validation, AGU Fall Meeting Abstracts.

Prakash, S., 2019. Performance assessment of CHIRPS, MSWEP, SM2RAIN-CCI, and TMPA precipitation products across India. Journal of hydrology, 571: 50-59.

Samra, J., 2004. Review and analysis of drought monitoring, declaration and management in India, 84. IWMI.

Schwarz, G., 1978. Estimating the dimension of a model. The annals of statistics, 6(2): 461-464.

Sharifi, E., Steinacker, R., Saghafian, B., 2016. Assessment of GPM-IMERG and other precipitation products against gauge data under different topographic and climatic conditions in Iran: Preliminary results. Remote Sensing, 8(2): 135.

Shen, Y., Xiong, A., Wang, Y., Xie, P., 2010. Performance of high-resolution satellite precipitation products over China. Journal of Geophysical Research: Atmospheres, 115(D2).

SIRDAŞ, S., Sen, Z., 2003. Spatio-temporal drought analysis in the Trakya region, Turkey. Hydrological Sciences Journal, 48(5): 809-820.

Stagge, J.H., Tallaksen, L.M., Gudmundsson, L., Van Loon, A.F., Stahl, K., 2015. Candidate distributions for climatological drought indices (SPI and SPEI). International Journal of Climatology, 35(13): 4027-4040.

Stisen, S., Sandholt, I., 2010. Evaluation of remote-sensing-based rainfall products through predictive capability in hydrological runoff modelling. Hydrological Processes: An International Journal, 24(7): 879-891.

Svoboda, M., Hayes, M., Wood, D., 2012. Standardized precipitation index user guide. World Meteorological Organization Geneva, Switzerland.

Tan, M., Ibrahim, A., Duan, Z., Cracknell, A., Chaplot, V., 2015. Evaluation of six high-resolution satellite and ground-based precipitation products over Malaysia. Remote Sensing, 7(2): 1504-1528.

Thom, H.C., 1958. A note on the gamma distribution. Monthly Weather Review, 86(4): 117-122.

Thomas, T., Jaiswal, R., Galkate, R., Nayak, T., 2016. Reconnaissance drought index based evaluation of meteorological drought characteristics in Bundelkhand. Procedia Technology, 24: 23-30.

Thomas, T., Nayak, P., Ghosh, N.C., 2015. Spatiotemporal analysis of drought characteristics in the bundelkhand region of central india using the standardized precipitation index. Journal of Hydrologic Engineering, 20(11): 05015004.

Umran Komuscu, A., 1999. Using the SPI to analyze spatial and temporal patterns of drought in Turkey. Drought Network News (1994-2001): 49.

Vicente-Serrano, S.M. et al., 2014. Evidence of increasing drought severity caused by temperature rise in southern Europe. Environmental Research Letters, 9(4): 044001.

Wei, W.W., 2006. Time series analysis, The Oxford Handbook of Quantitative Methods in Psychology: Vol. 2.

Wilhite, D.A., 2000. Drought as a natural hazard: concepts and definitions.

Wilhite, D.A., Glantz, M.H., 1985. Understanding: the drought phenomenon: the role of definitions. Water international, 10(3): 111-120.

673 Wilson, G.T., 1989. On the use of marginal likelihood in time series model estimation. Journal of
674 the Royal Statistical Society: Series B (Methodological), 51(1): 15-27.
675 Xie, P. et al., 2007. A gauge-based analysis of daily precipitation over East Asia. Journal of
676 Hydrometeorology, 8(3): 607-626.
677 Yang, Y., Luo, Y., 2014. Evaluating the performance of remote sensing precipitation products
678 CMORPH, PERSIANN, and TMPA, in the arid region of northwest China. Theoretical
679 and applied climatology, 118(3): 429-445.
680 Zhao, H., Ma, Y., 2019. Evaluating the Drought-Monitoring Utility of Four Satellite-Based
681 Quantitative Precipitation Estimation Products at Global Scale. Remote Sensing, 11(17):
682 2010.

683
684